

Optical properties of heavily boron-doped nanocrystalline diamond films studied by spectroscopic ellipsometry

Non Peer-reviewed author version

Zimmer, A.; WILLIAMS, Oliver; HAENEN, Ken & Terryn, H. (2008) Optical properties of heavily boron-doped nanocrystalline diamond films studied by spectroscopic ellipsometry. In: APPLIED PHYSICS LETTERS, 93(13).

DOI: 10.1063/1.2990679

Handle: <http://hdl.handle.net/1942/8569>

Optical Properties of Heavily Boron-doped Nanocrystalline Diamond Films Studied by Spectroscopic Ellipsometry

A. Zimmer^{1,*a)}, O. A. Williams^{2,3}, K. Haenen^{2,3}, H. Terryn¹

1 - Research Group Metallurgy, Electrochemistry and Materials Science, Vrije Universiteit Brussel, Belgium

2 - Institute for Materials Research (IMO), Universiteit Hasselt, Diepenbeek, Belgium

3 - Division IMOMEC, IMEC vzw, Diepenbeek, Belgium

^{a)}Electronic mail : alex.zimmer@ellipsometrie.fr

*Current affiliation: Research Group Electrochimie Interfaciale - Corrosion, Institut Carnot de Bourgogne, UMR 5209 CNRS-Université de Bourgogne, Dijon, France

The optical properties of heavily boron-doped nanocrystalline diamond films grown by microwave plasma enhanced chemical vapor deposition on silicon substrates are presented. The diamond films are characterized by spectroscopic ellipsometry within the mid-infrared, visible and near-ultraviolet regions. The ellipsometric spectra are also found to be best described by a four-phase model yielding access to the optical constants which are found distinct from previous nanocrystalline diamond literature values. The presence of a subgap absorption yielding high extinction coefficient values defined clearly the boron incorporated films in comparison to both undoped and composite films, while refractive index values are relatively comparable.

At present, nanocrystalline diamond (NCD) films are attracting substantial interest. As such films can be deposited on a plethora of materials,¹ possible applications include NEMS and MEMS structures,² biosensors,³ tribology,⁴ optical coatings⁵ and thermal management.⁶ By adding boron, NCD films can be turned into a p-type semiconductor. Conductivity values can be tuned within 11 orders of magnitude, with values ranging between $1 \times 10^{-9} \Omega^{-1}\text{cm}^{-1}$ and $100 \Omega^{-1}\text{cm}^{-1}$.⁷ The latter films show a metallic conductivity behavior, even turning superconducting when cooled down to sufficient low temperature ($\sim 3\text{K}$).⁸

Spectroscopic Ellipsometry (SE) is a non-destructive optical method which measures the complex ratio R of the Fresnel reflection coefficients of particular directions polarized light (r_p , r_s) and reports the ratio in terms of the ellipsometric angles Ψ and Δ defined by the equation:⁹

$$R = r_p / r_s = \tan \Psi e^{j\Delta} \quad (1)$$

Both *ex* and *in situ* SE for optical characterization of diamond thin films have been used by Collins *et al.* in the beginning of the '90s.¹⁰⁻¹¹ SE has also begun to be a powerful technique for microcrystalline diamond films.¹²⁻¹⁵ Concerning NCD films, reports have just appeared over the last few years.¹⁶⁻¹⁹ Recently the team of Popov optically characterized NCD/a-C composite films prepared by MWCVD including SE in the range 250-860 nm.¹⁷ Results were compared with those of polycrystalline films. The use of a Tauc-Lorentz dispersion relation²⁰ in the optical model yields one low value of bandgap ($E_g \sim 1.4 \text{ eV}$). Z.G. Hu *et al.*¹⁹ used also SE to analyze NCD films with a four phase model in the range 260-1130 nm. The use of a Sellmeier dispersion relation allows authors to determine the lowest direct bandgap with an approximation (6.9 eV). As for the microcrystalline case, authors propose successive models in order to improve the match between experimental and fitted data for the nanocrystalline case. This match defines the mean squared error χ^2 which is a criterion to determine the accuracy of the optical model. However, χ^2 does not verify the physical correctness of the model. The support of other characterization techniques is then necessary to build up a reliable model, in order to minimize the range of mathematical solutions in fitting procedure. In this letter, SE has been applied to obtain further information about both optical and morphological properties of B-NCD/Si films. SEM and particularly total Reflection measurements have been used to determine the validity of the model.

Nanocrystalline diamond films of different thicknesses were grown on silicon wafers by a microwave plasma chemical vapour deposition process using an ASTeX 6500 reactor. Before

growth, the Si wafers were pretreated using monodisperse nanodiamond aqueous colloid, leading to very high nucleation densities.²¹ The gas flow rate, gas pressure, microwave power and substrate temperature were 485 sccm H₂, 15 sccm CH₄, 35 Torr, 3500 W, and 700 °C respectively. In addition, all films were doped with boron by adding trimethylboron (TMB) to the gas mixture in a ~ 6500 ppm [TMB]/[H₂] ratio. This concentration leads to a large boron incorporation, leading to metallic-like conduction⁷ and even superconductivity when cooled sufficiently.⁸ To study the influence of the film thickness the deposition time of film 2-70406 (100 minutes) was 5 times higher than that of 2-70313 (20 minutes).

Coloration rises in the analyzed boron doped NCD (B-NCD) films: a transition from purple (thinnest film 2-70313) to grey (thickest film 2-70406) is observed. In order to investigate their spectral appearance, experimental colors were measured with a spectrophotometer (Ultrascan XE from Hunterlab). It is based upon an integrated sphere geometry and a D65/10–light source. The measurements were conducted in the 360–750 nm wavelength range. Figure 1 (points) shows the experimental spectra of total reflection for film 2-70313. Corresponding colors can be calculated by means of the 1976 norm of the Commission Internationale de l'Éclairage (CIE) in the L*a*b*-system where the L* coordinate gives the variation from white (100%) to black (0%), a* gives the variation from green (+) to red (-) and b* the variation from blue (+) to yellow (-). For example, the purple colored film corresponds to L*=23.62, a*=23.24 and b*=-20.83. The ellipsometric measurements were performed in a spectral range of 0.03–4.3 eV at three angles of incidence (60–65–70°) with two ellipsometers from J.A. Woollam Co, Inc. and analyzed with the WVASE32 software. Figure 2 (dashed line) shows the experimental (Ψ, Δ) spectra obtained for the thinnest film. Artifacts near 0.9 eV correspond to overlapping of the two ellipsometers ranges. After an initial step of fitting data with several basic models from the literature (not shown here), two four-phase models gave good overall matches: air/surface rough layer/B-NCD film/Si substrate. For both cases, the dielectric function of the bulk component of B-NCD films was determined by a global fit in the whole spectroscopic range and modeled by combining a Lorentz oscillator (parameters are peak position L.E1, broadening L.Br1 and amplitude L.A1) for the IR part with: (i) a Tauc-Lorentz oscillator (peak position TL.En, broadening TL.C, amplitude TL.A and bandgap TL.Eg, Model 1) or (ii) a second Lorentz oscillator (L.E2, L.Br2, L.A2, Model 2) for the UV-VIS part. The dielectric function of the substrate is obtained experimentally by

inversion of the ellipsometric angles. The surface rough layer (top layer thickness, NCD/void fraction) is commonly simulated by effective medium theory of Bruggeman.²²

The best fitted curves of film 2-70313 are shown in the Fig. 2 (a) and (b) (lines) for Model 1. Best-fit parameters are illustrated in Table I. Considering only χ^2 values Model 2 was found to be more suitable than the first one (lower χ^2 value). Among the energy parameters, the average UV-VIS peak position LE1 of Model 2 is about 10.5 eV indicating that the fundamental bandgap E_g is over the experimentally available energy maximum of 4.3 eV. This is also the case in Model 1 which gives directly an average value of bandgap of 7 eV. The difference with Boycheva *et al.*¹⁷ on a-C/NCD film (1.4 eV) is due to an amorphous carbon feature. Moreover their determination of E_g was done graphically via a Tauc plot and the fitted value of E_g was not shown although it was obtained with a Tauc-Lorentz parameterization. In our case of quasi amorphous carbon free B-NCD films, E_g approaches the lowest direct optical bandgap of single-crystal diamond (7.2 eV) like another estimation done by Hu *et al.*¹⁹ on undoped NCD films. The dispersion relations also indicate a subgap absorption in the mid infrared region which will be discussed in the next paragraph. For this IR oscillator, both models give close parameters. Among the morphological parameters, the total thickness of the B-NCD films is found to vary between 75 and 383 nm (Model 1) or 74 and 469 nm (Model 2). A check of the thickness was done by SEM measurements on cross-sections. For the thinnest film, both models agree with SEM value (about 80 nm, Fig. 3 (a)) while Model 2 overestimates the thickness for the thickest one (about 350 nm by SEM, Fig. 3 (b)). Another check is given by the color difference ΔE^* which is another description of the difference between the experimental and the generated data (in terms of L^* , a^* , b^*):

$$\Delta E^* = \sqrt{\Delta L^{*2} + \Delta a^{*2} + \Delta b^{*2}} \quad (2)$$

The lower this value, the better both colors match. If there is a very good agreement between the color generated from the model and the experimentally measured color, it can be concluded that optical model is physically justified. By testing this procedure with both models, Model 1 appeared finally the more physically correct (lower ΔE^* values, Table I). Figure 1 (line) also shows the generated reflection spectra obtained from Model 1 which matches well the experimental spectra. The color of the surface and the thickness of the film, both confirmed by additional techniques, could also be predicted by ellipsometry (Model 1). Concerning surface

roughness, the void fractions appear slightly dependent of the bulk thickness (32%, 35%) while top layer thicknesses (32 nm, 50 nm) confirm the increase of roughness with bulk thickness.¹ Figure 4 gives the refractive index n and extinction coefficient k of the B-NCD films, grown with different deposition times. The refractive index of B-NCD films 2.7-2.2/2.8-2.0 are close to that of recent undoped¹⁹ (~ 2) and composite¹⁶ (2.5-2.4) NCD films but high absorption in the IR is found, yielding unusually high extinction coefficients in the VIS-NIR. This can be explained by the high boron content in the films. It is known that boron induces an acceptor level at 0.37 eV (~ 3450 nm) leading to increased light absorption for higher energies.^{1,23} The fitted peak position of Lorentz oscillator is found near to this value. Some variations are also observed between the two samples. Even if the thinnest film gave a reasonable good fit, further improvements could be necessary for the thicker one to clarify the influence of the deposition time on the optical functions of B-NCD films.

In summary, SE experiments have been applied to B-NCD films and a straightforward analysis was obtained with the thinnest sample. Validity of the best-fit parameters has been verified qualitatively with color simulations and SEM. These films possess well-defined optical properties: UV-VIS refractive indexes close to that of recent undoped and composite NCD films, unusual non-zero extinction coefficients due to high boron subgap absorption present in IR and high bandgap approaching the lowest direct electronic transition of single-crystal diamond.

Acknowledgments

This work was financially supported by the EU FP6 Marie Curie RTN “DRIVE” (MRTN-CT-2004-512224), by the Research Programs G.0068.07 and G.0430.07 of the Research Foundation - Flanders (FWO), and the IAP-P6/42 project “Quantum Effects in Clusters and Nanowires”. KH is a Postdoctoral Fellow of the Research Foundation - Flanders (FWO).

The authors thank L. Zhang, R. Erni and G. Van Tendeloo (EMAT, Universiteit Antwerpen, Belgium) for the SEM pictures.

References

- ¹ O. A. Williams, M. Nesládek, *physica status solidi (a)*, 203/13, 3375 (2006).
- ² O. A. Williams, V. Mortet, M. Daenen, K. Haenen, *Applied Physics Letters* 90/6, 063514 (2007).
- ³ V. Vermeeren, N. Bijmens, S. Wenmackers, M. Daenen, K. Haenen, O.A. Williams, M. Ameloot, M. van de Ven, P. Wagner, L. Michiels, *Langmuir* 23/26, 13193 (2007).
- ⁴ A.V. Sumant, A.R. Krauss, D.M. Gruen, O. Auciello, A. Erdemir, M. Williams, A.F. Artiles, W. Adams, *Tribology transactions*, 48, 1, 24 (2005).
- ⁵ P. Achatz, J. A. Garrido, M. Stutzmann, O. A. Williams, D. M. Gruen, *Applied Physics Letters* 88, 101908 (2006).
- ⁶ J. Philip, P. Hess, T. Feygelson, J. E. Butler, S. Chattopadhyay, K. H. Chen, L. C. Chen, *Journal of Applied. Physics* 93, 2164 (2003).
- ⁷ O.A. Williams, M. Nesládek, M. Daenen, S. Michaelson, A. Hoffman, E. Osawa, K. Haenen, R.B. Jackman, *Diamond & Related Materials* 17, 1080 (2008).
- ⁸ M. Nesládek, D. Tromson, C. Mer, P. Bergonzo, P. Hubik, J.J. Mares, *Applied Physics Letters* 88, 232111 (2006).
- ⁹ R.M.A. Azzam and N.M. Bashara, *Ellipsometry and Polarized Light*, North-Holland, New York (1977).
- ¹⁰ Y. Cong and R.W. Collins, *Appl. Phys. Lett.*, 58, 2, 819 (1991).
- ¹¹ R.W.Collins, Y.Cong, H.V. Nguyen, I.An, K.Vedam, T.Badzian, R.Messier, *J.Appl. Phys.* 71, 10, 5287 (1992).
- ¹² N. Cella, H. El Rhaleb, J.P. Roger, D. Fournier, E. Anger, A. Gicquel, *Diamond and Related Materials*, 5, 1424 (1996).

- ¹³ I. Pinter, P. Petrik, E. Szilágyi, Sz. Kátai, P. Deák, *Diamond and related materials*, 6, 1633 (1997).
- ¹⁴ G. Fedosenko, D. Korzec, J. Engemann, D. Lyebyedyev, H.C. Scheer, *Thin Solid Films*, 406, 275 (2002).
- ¹⁵ Z. Fang, Y. Xia, L. Wang, W. Zhang, Z. Ma, M. Zhang, *carbon*, 41, 967 (2003).
- ¹⁶ T. Guzdek, J. Szmidt, M. Dudek, P. Niedzielski, *Diamond and related materials*, 13, 1059 (2004).
- ¹⁷ S. Boycheva, C. Popov, J. Bulir, A. Piegari and W. Kulisch, *Fullerenes, Nanotubes, and Carbon Nanostructures*, 13 (S1), 457 (2005).
- ¹⁸ L-J. Wang, L-w. Jiang, L. Ren, J-m. Liu, Q-f. Su, R. Xu, H-y. Peng, W-m. Shi and Y-b. Xia, *Trans. Nonferrous Met. Soc. China*, 16, s289 (2006).
- ¹⁹ Z. G. Hu, P. Prunici, P. Hess and K. H. Chen, *J Mater Sci: Mater Electron*, 18, S37 (2007).
- ²⁰ G. E. Jellison, Jr., and F. A. Modine, *Appl. Phys. Lett.*, 69, 371 (1996); and Erratum, *Appl. Phys. Lett.*, 69, 2137.15 (1996).
- ²¹ O.A. Williams, O. Douhéret, M. Daenen, K. Haenen, E. Osawa, M. Takahashi, *Chemical Physics Letters* 445, 255 (2007).
- ²² D.A.G. Bruggeman, *Ann. Phys.* 24, 636 (1935).
- ²³ D. Wu, Y.C. Ma, Z.L. Wang, Q. Luo, C.Z. Gu, N.L. Wang, C.Y. Li, X.Y. Lu, Z.S. Jin, *Phys. Rev. B*, 73, 012501 (2006).

Tables

TAB. I. Summary of best fit parameters for both models and corresponding selection criteria (χ^2 : mean square error and ΔE^* : color difference).

Model	1	1	2	2
Film	2-70313	2-70406	2-70313	2-70406
Top layer (nm)	32.4	49.5	29.1	42.7
NCD fraction	0.68	0.65	0.73	0.68
Bulk layer (nm)	42.7	333	45.2	426
L.E1 (eV)	0.288	0.146	0.29	0.09
L.A1	150	285	133	713
L.Br1 (eV)	1.76	1.08	1.72	1.07
TL.En/L.E2 (eV)	7.50	8.42	8.70	12.3
TL.A/L.A2	1470	5690	5.3	5.2
TL.C/L.Br2 (eV)	1.24	0.46	0.45	2.9
TL.Eg (eV)	6.67	7.43		
χ^2	2.51	7.52	2.32	3.43
ΔE^*	1.06	8.54	13.8	10.1

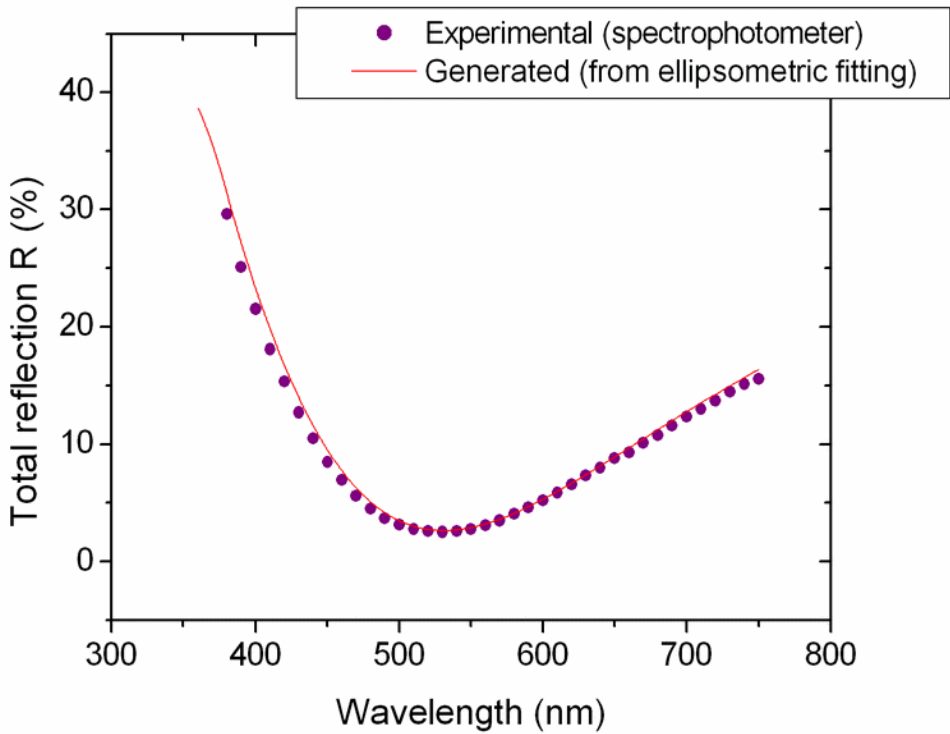
List of figure captions

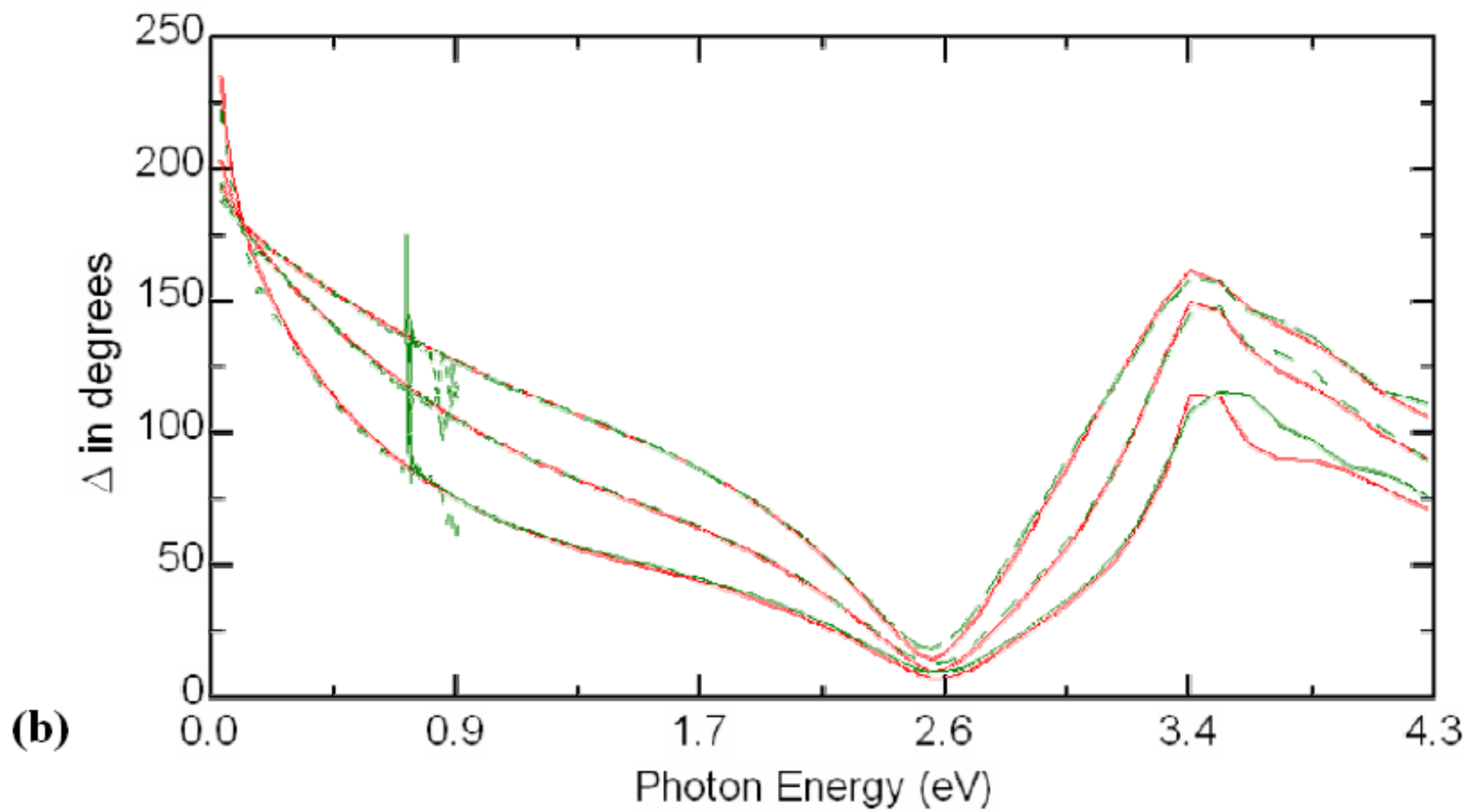
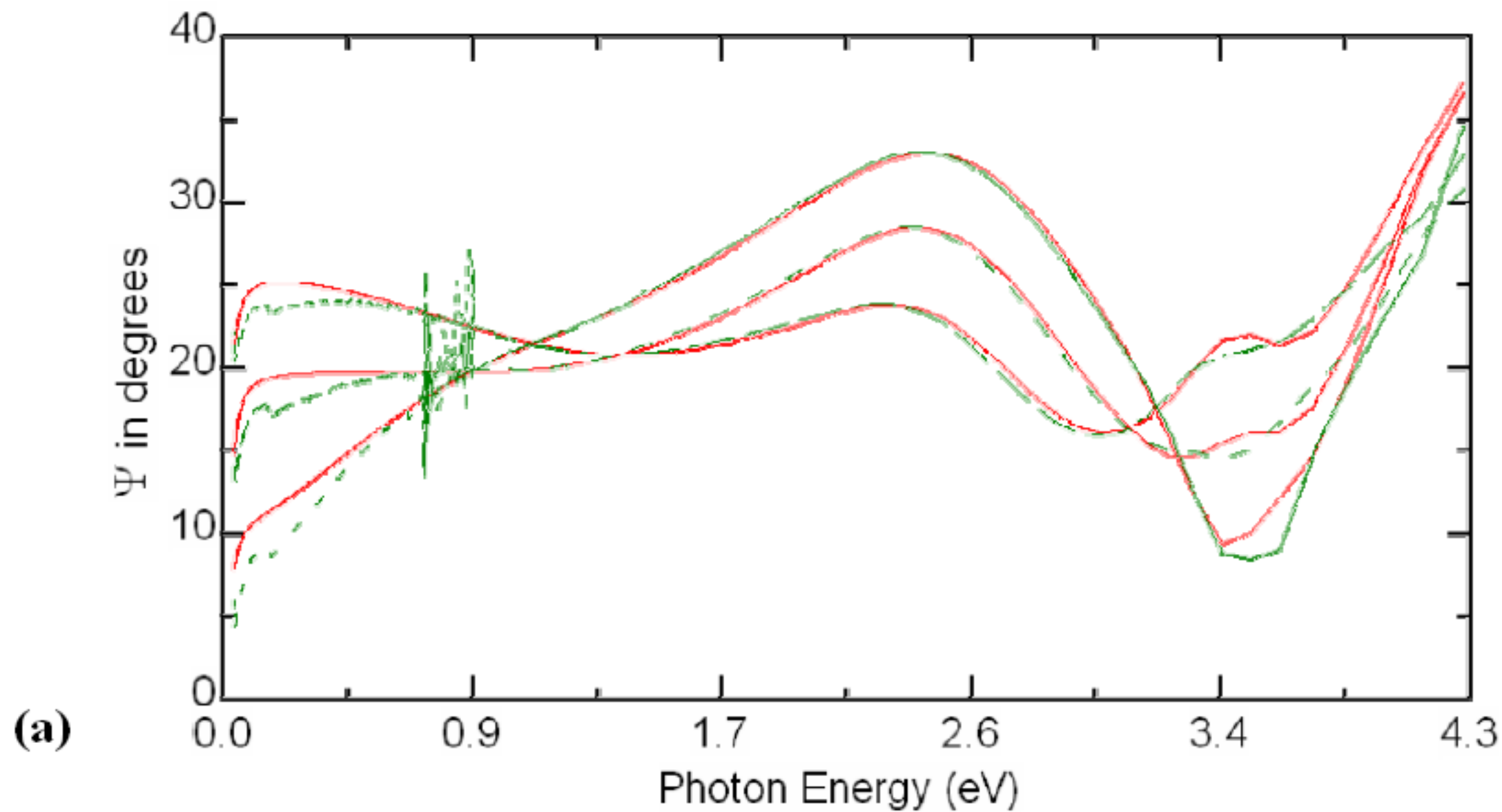
FIG. 1. Experimental (points) and generated (line) spectra of total reflection vs wavelength of the B-NCD film (film 2-70313).

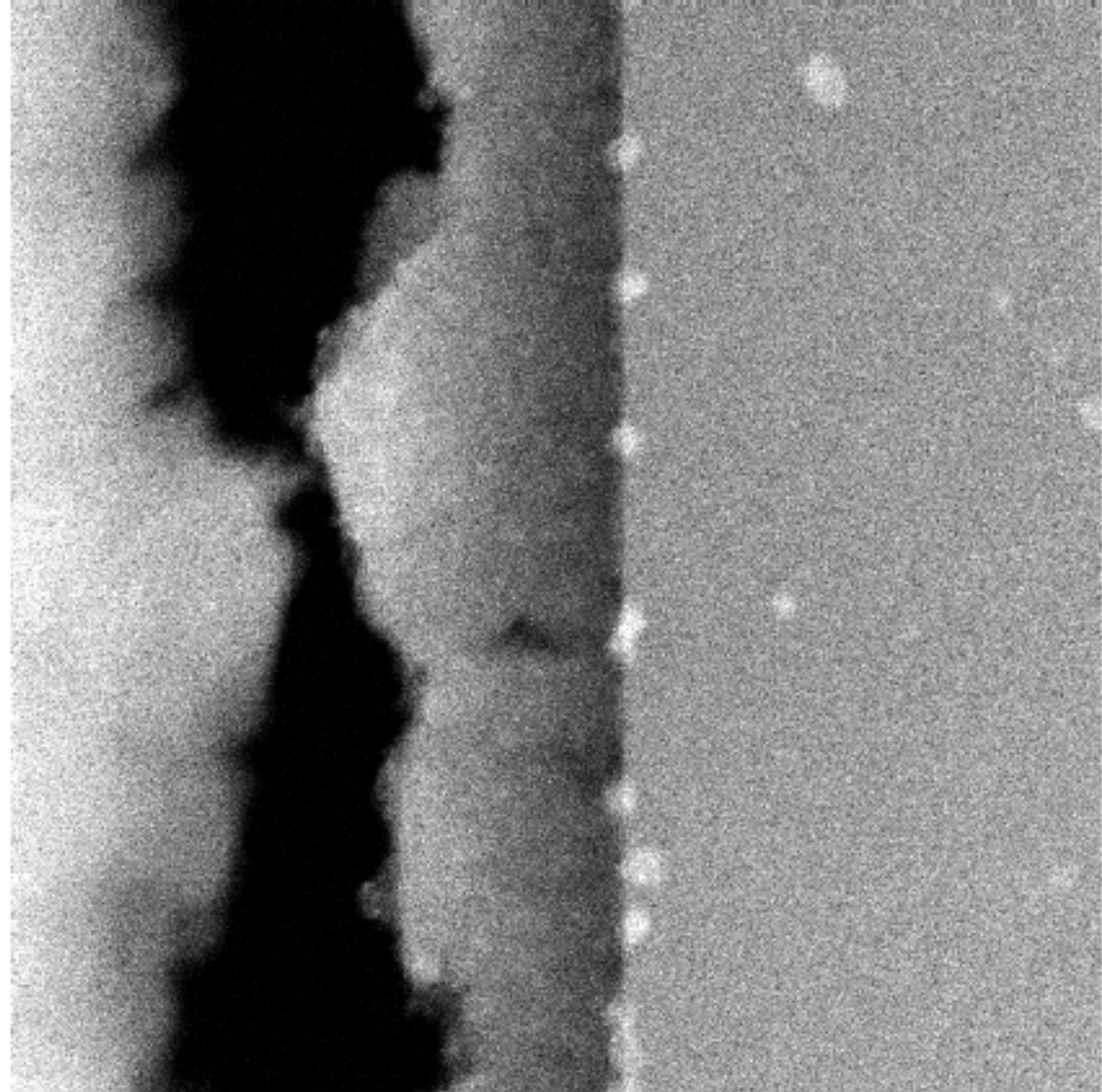
FIG. 2. Ellipsometric spectra vs energy of the B-NCD film (film 2-70313): (a) experimental Ψ (dashed line) and fitted (line) Ψ from Model 1. (b) experimental Δ (dashed line) and fitted (line) Δ from Model 1. The three curves correspond to the three employed angles of incidence (65-70-75°).

FIG. 3. SEM images: (a) film 2-70313. (b) film 2-70406.

FIG. 4. Complex index of refraction of B-NCD films vs wavelength.

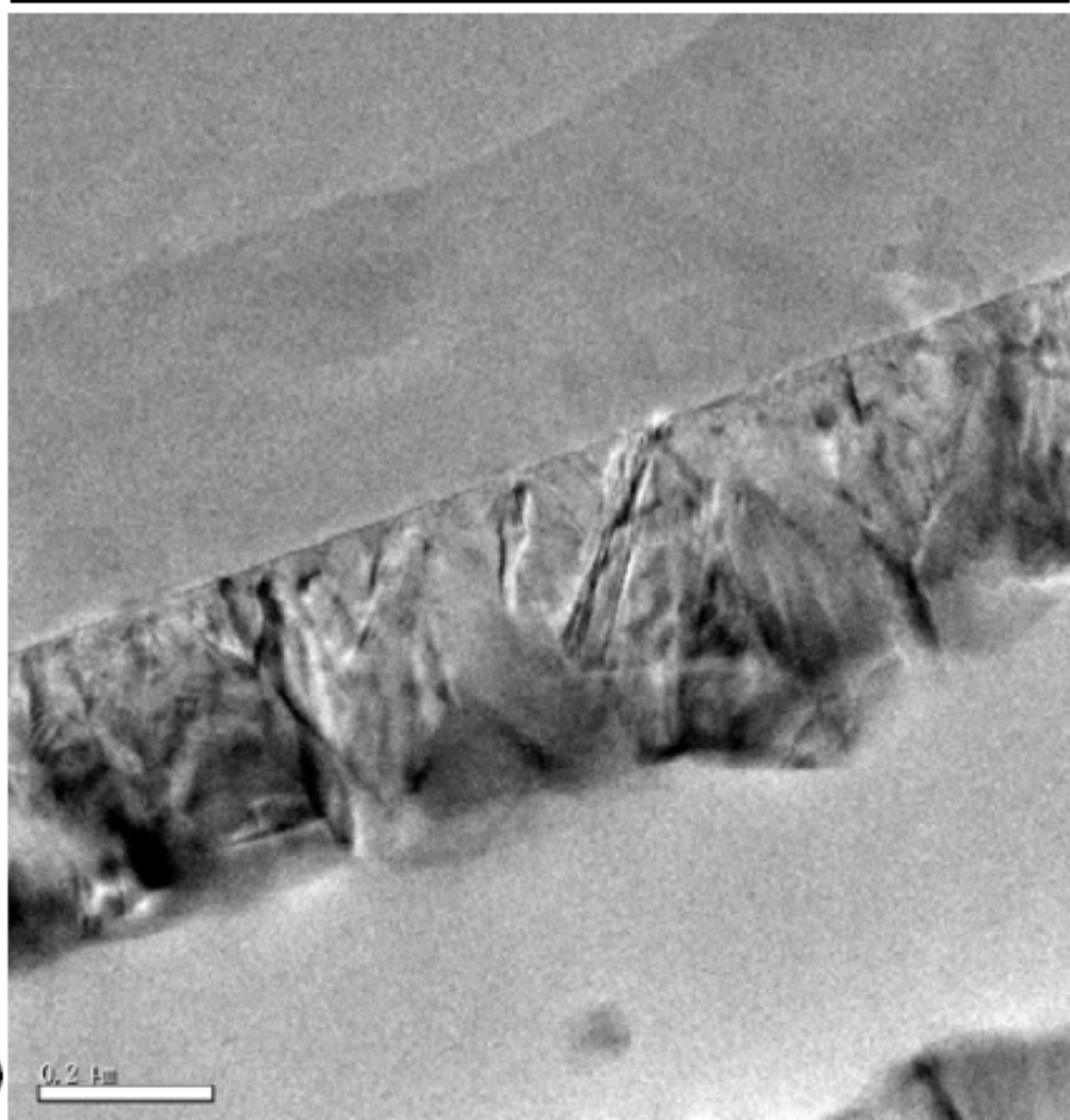






(a)

50 nm



(b)

0.2 nm

